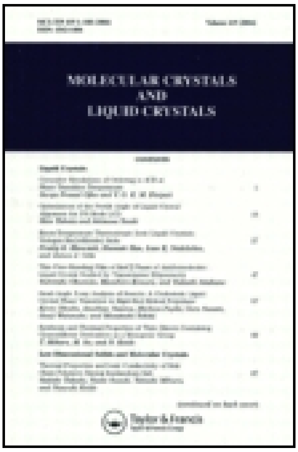

Molecular Crystals and Liquid Crystals Science and Technology. Section A. Molecular Crystals and Liquid Crystals
Publication details, including instructions for authors and subscription information:
http://www.tandfonline.com/loi/gmcl19

Surface Effect on the Threshold Electric Fields of Cholesteric-Nematic Phase Transition and Its Reverse Process

Akihiro Mochizuki [a] & Shunsuke Kobayashi [b]
[a] Fujitsu Laboratories Ltd, Atsugi, Kanagawa, Japan
[b] Tokyo University of Agriculture and Technology, Koganei, Tokyo, Japan
Version of record first published: 24 Sep 2006.

To cite this article: Akihiro Mochizuki & Shunsuke Kobayashi (1993): Surface Effect on the Threshold Electric Fields of Cholesteric-Nematic Phase Transition and Its Reverse Process, Molecular Crystals and Liquid Crystals Science and Technology. Section A. Molecular Crystals and Liquid Crystals, 225:1, 89-98

To link to this article: http://dx.doi.org/10.1080/10587259308036220

Mol. Cryst. Liq. Cryst., 1993, Vol. 225, pp. 89–98
Reprints available directly from the publisher
Photocopying permitted by license only

Printed in the United States of America

Surface Effect on the Threshold Electric Fields of Cholesteric-Nematic Phase Transition and Its Reverse Process

AKIHIRO MOCHIZUKI*
Fujitsu Laboratories Ltd. Atsugi, Kanagawa, Japan

and

SHUNSUKE KOBAYASHI
Tokyo University of Agriculture and Technology Koganei, Tokyo, Japan

(Received March 10, 1992; in final form May 1, 1992)

Electric-field-induced cholesteric-nematic (Ch-N) phase transition and its reverse process (N-Ch) are discussed by taking account of the surface interaction effect. Threshold electric fields of a cholesteric to nematic and a nematic to cholesteric phase transition are investigated in conjunction with a liquid crystal layer thickness and surface anchoring strength. By performing a fitting of the theoretical curves to the experimental results of the threshold electric field strengths, we concluded that in a homeotropically aligned thin cell whose liquid crystal layer thickness is below 10 μm, the surface anchoring energy, A_0, contributes significantly to reduce the threshold electric fields both for the Ch-N phase transition and that of N-Ch.

Keywords: Cholesteric, Nematic, Phase transition, Surface interaction, Anchoring energy

1. INTRODUCTION

The electrically induced cholesteric-nematic phase transition is a well known phenomenon, and it has been used for several types of liquid crystal displays such as light scattering,[1,2] the White-Taylor[3] type and a bistable memory type.[4–6] There have been several reports on the cholesteric-nematic phase transition phenomenon.[7,8] The threshold electric field from the cholesteric to nematic (Ch-N) phase was derived by de Gennes and Meyer independently, and that of Ch-N was derived by Greubel and they discussed the dependence on the elastic constants and the helical pitch of the liquid crystal material.[9,10] In these preceding papers, the thickness of the liquid crystal layer and the surface anchoring strength, however, have

*A. Mochizuki is also in the Division of Electronic and Information Engineering of the Graduate School of Technology, Tokyo University of Agriculture and Technology.

been considered to give a small contribution to these threshold field strengths. Lee *et al.* recently published the effect of homeotropic surface anchoring on the cholesteric to nematic phase transition.[11] They discuss the surface effect from the view point of the interaction of helical pitch and liquid crystal layer thickness. Van Sprang also described the electrically induced Ch-N phase transition, taking into account surface interaction.[12]

We have investigated the bistable memory effect of the electric field induced Ch-N phase transition phenomenon for the application to a projection display utilizing the light scattering effect.[13-15] In the course of the investigation of the bistable memory effect, we have found experimentally that both the threshold fields Ch to N and N to Ch are strongly dependent on a cell gap. Particularly when a cell gap is less than around 10 μm, the threshold electric field strength shows a decrease with the decrease of the cell gap. In this paper we will show first experimentally how the electric-field-induced Ch-N phase transition effect, in particular threshold voltage, is influenced by the surface anchoring effect; then we will give a theoretical explanation for this phenomenon based on a simple model.

2. EXPERIMENTAL

A cholesteric (Ch) phase LC material was prepared by mixing a nematic (N) LC mixture (RO-TN-403: Roche) and the chiral nematic LC (CB-15: Merck Ltd.) as a dopant. Two types of LC mixtures whose helical pitches are 0.9 μm and 1.5 μm, respectively, were prepared by changing the mixing ratio of the chiral dopant.

The surfaces of the ITO coated and patterned glass plates were treated by N, N-dimethyl-N-octadecyl-3-aminopropyltrimethoxysilyl chloride (DMOAP) to provide a homeotropic alignment. To investigate the influence of the surface effect on the threshold, LC panels with cell gaps ranging from 1.6 μm to 20 μm were prepared using silica balls as a spacer segment, with an accuracy of ±0.2 μm over the sample cell. The cell thickness was measured interferometrically.

The threshold electric field was measured by applying a triangular electric voltage waveform at 0.05 Hz. The LC panel was set between crossed polarizers, and the light transmittance was plotted as a function of the applied voltage using parallel white light. We measured the transmittance change using crossed polarizers for obtaining a clear threshold voltage. The electric field which gives rise to 90% transmittance in the phase transition from Ch to N was defined as the threshold electric field, E_{CN}; while the electric field for the N to Ch transition was defined as the threshold electric field, E_{NC}. All of the threshold field measurements were done at 25°C.

3. RESULTS AND DISCUSSION

3.1 Cholesteric to Nematic Phase Transition

An electric-field-induced phase transition from a Ch to an N is known to be expressed as

$$E_{CN} = \frac{\pi^2}{P_0}\sqrt{\frac{K_{22}}{\varepsilon_0 \Delta\varepsilon}} \tag{1}$$

by de Gennes,[16] where E_{CN} is the threshold electric field from Ch to N transition, P_0 is the helical pitch in the absence of the electric field, K_{22} is the elastic constant of twist, ε_0 is the vacuum permitivity, and $\Delta\varepsilon$ is the dielectric anisotropy of the LC. In the derivation of E_{CN}, equation (1) for E_{CN}, no surface anchoring effect is taken account of. Equation (1) does not contain any quantities relevant to the surface anchoring such as the polar anchoring strength and the thickness of the LC medium. However experimentally we sometimes observe that the threshold field varies with both the cell thickness and the condition of the surface treatment. Van Sprang reported the influence of the surface interaction on the threshold fields in the Ch-N phase transition using an oblique evaporation of silicon mono-oxide.[12]

Goosense discussed that the homeotropic surface treatment assists the electric-field-induced unwinding in the final stage, while the homogeneous treatment opposes this phenomenon. The cell thickness dependence and the surface treatment of the threshold field may suggest that the surface interaction between the liquid crystal medium and the orientation layer should have some influence on the threshold field.

The helical structure of the cholesteric phase liquid crystal for a homeotropically treated LC panel is elucidated in Figure 1. When the cell thickness d is large enough, for example 100 μm, the effect of the variation of the molecular conformation from the surface region to that of the bulk region may be negligibly small and the helical structure with an axis directing parallel to the normal of the substrate may be firmly constructed in the bulk region.

However, when the cell thickness is small, say several μms then the surface anchoring effect may play a role in modifying the threshold field E_{CN}, since the surface anchoring energy cannot be neglected relative to the bulk distorsion energy in the course of the unwinding of the helix that causes Ch-N transition. The experimental results using 0.9 μm and 1.5 μm pitch LC cells are given by Figures 2 and 3, respectively. Both results clearly show, first, that the threshold field tends to saturate for the thick cells over 20 μm; and second, decreases with decrease of the cell gaps. The comparison of the results of Figures 2 and 3 indicates that the

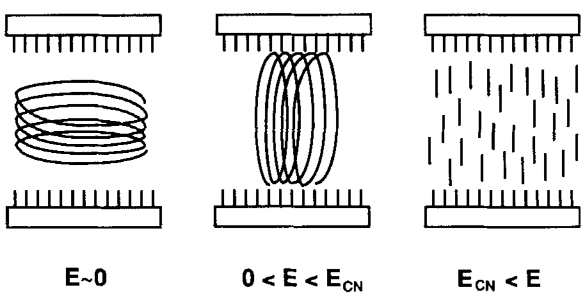

FIGURE 1 Variation of the molecular conformation in the course of the cholesteric-nematic phase transition. When the externally applied electric field strength is low, the helical axis of the liquid crystal is perpendicular to the substrates even though the vertical surface alignment is done. The increase of the applied field leads the helical axis rotation to be parallel to the substrates, as shown in the second phase. Finally, the field strength exceeds a threshold value, the helical structure disappeared and all of the liquid crystal molecules tend to align parallel to the field. The final state is the field-induced nematic phase that is transparent.

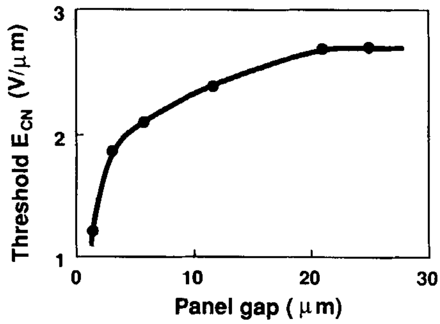

FIGURE 2 The variation of the threshold electric field strengths, E_{CN}: with the LC layer thickness in the cholesteric to nematic phase transition of the homeotropically aligned 0.9 μm pitch cell.

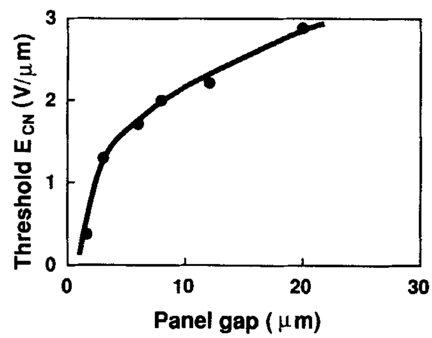

FIGURE 3 The variation of the threshold electric field strengths, E_{CN}: with the LC layer thickness in the cholesteric to nematic phase transition of the homeotropically aligned 1.5 μm pitch cell.

dependence of the threshold field on the cell gap for the LC cell with a longer pitch (Figure 3) is stronger than that of the cell with a shorter pitch (Figure 2). These phenomena may be explained by considering the difference in the relative contribution of the surface anchoring energy to the whole energy to unwind the helical structure. The influence of the anchoring energy in the longer pitch cell may be stronger than that in the shorter pitch cell. Thus, the cell-gap dependence of the threshold field is stronger in the longer pitch panel.

In the longer pitch panel, the threshold field of the 1.6 μm cell is so small that it is less than 0.4 V/μm. However, it is assumed that the 1.6 μm cell is too narrow to maintain the 1.5 μm helical pitch structure. In this panel, the liquid crystal should be strongly distorted. Thus in this panel, the effective elastic constant and the effective helical pitch are assumed to be modulated.

The threshold field, E_{CN}, which takes account of the surface effect, may be expressed as

$$E_{CN}^{*} = \sqrt{E_{CN}^{2} - \frac{2A_{\theta}}{\varepsilon_0 \Delta\varepsilon (d - \xi)}}, \tag{2}$$

where A_θ is a surface anchoring energy, d is a cell gap and ξ is the thickness of the unwound layer of the helical structure. The derivation of Equation (2) is given in the appendix. Equation (2) indicates that when the surface anchoring is strong and the cell gap is small, the threshold field of the Ch-N becomes small. This means that the homeotropic surface anchoring plays a role in accelerating the final unwinding.

Figure 4 shows an example of the dependence of the experimental values of threshold fields on the cell gap and theoretical fittings using Equation (2); a fairly good agreement with the experimental result is obtained by choosing $A_\theta = 5 \times 10^{-4}\,\mathrm{J/m^2}$, $E_{CN} = 2.8 \times 10^6$ V/m, $\xi = 1$ μm, and $\Delta\varepsilon = 10$. The value of A_θ is in good agreement with other independent experiments. The value of ξ was determined by observing the occurrence of the unwinding in a very narrow gap cell.

This curve fitting suggests that the surface anchoring effect is quite significant when the cell gap is smaller than 5 μm. However, when the cell gap is larger than 20 μm, the anchoring effect on the phase transition is almost negligible, and the expression derived by de Gennes (Equation 1) becomes useful only in this region.

3.2 Nematic to Cholesteric Phase Transition

For the N to Ch phase transition, Greubel has derived that for $K_{22} \geqslant (P_0/d)K_{33}$ the threshold E_{NC} can be expressed as

$$E_{NC} = \frac{\pi}{P_0}\sqrt{\frac{4K_{22}^2 - \left(\frac{P_0 K_{33}}{d}\right)^2}{\varepsilon_0 \Delta\varepsilon K_{33}}}, \tag{3}$$

where K_{33} is the bend elastic constant.[17] The derivation of Equation (3) was also done by neglecting the surface anchoring effect.

In this transition, the cell gap influence on the threshold field is already taken into account in Equation (3). Equation (3) indicates that the threshold field E_{NC} increases with the increase of cell gap, d.

The experimental results are roughly in accordance with Equation (3). However both Figures 5 and 6 show a minimum value when the cell gap is around 3 μm.

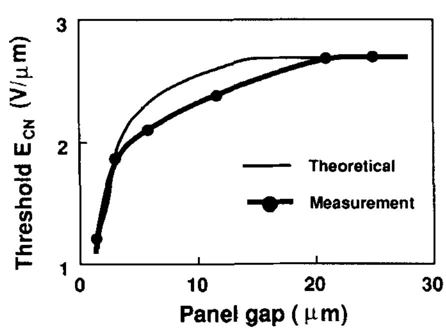

FIGURE 4 The theoretical and experimental results of the cholesteric to nematic phase transition field (0.9 μm pitch cell). In a thin thickness region, it is obvious that the surface interaction effect on the threshold field is significant.

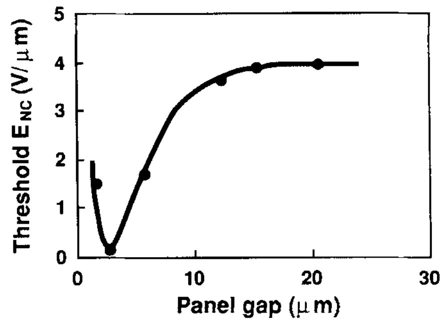

FIGURE 5 The threshold electric field strength, E_{NC}: nematic to cholesteric phase transition of the homeotropically aligned 0.9 μm pitch liquid crystal cell.

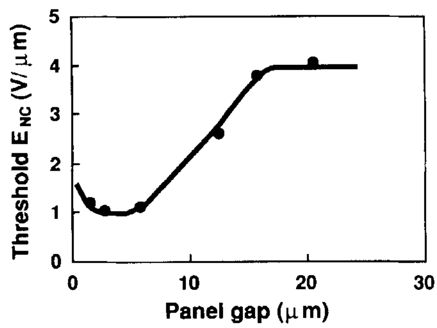

FIGURE 6 The threshold electric field strength, E_{NC}: nematic to cholesteric phase transition of the homeotropically aligned 1.5 μm pitch liquid crystal cell.

As described before in a thin gap region, the liquid crystal helical structure is strongly distorted by the surface effect. Therefore, in the thin gap region which is comparable to the helical structure, the elastic constants are assumed to be modified. Particularly, the twist elastic constant, K_{22}, is thought to decrease with the decrease of cell gap d. When $2K_{22} - P_0K_{33}/d$ is minimum, the threshold field, E_{NC}, shows a minimum value as shown in Figures 5 or 6. Further in a thin gap region, the twist elastic constant may be stronger again due to the relatively strong surface effect. The specific balance between the helical pitch and the cell gap governs the effective twist elastic constants. Therefore, the short pitch cell effects the surface effect strongly in the thin gap region. However, in the thick gap region, the relative surface effect is so small that it does not change the twist elastic constant.

Thus, in the nematic to cholesteric phase transition, the threshold field, E_{NC}, may be expressed as

$$E^*_{NC} = \frac{\pi}{P_0}\sqrt{\frac{4K^{*2}_{22} - \left(\frac{P_0K_{33}}{d}\right)^2}{\varepsilon_0\Delta\varepsilon K_{33}}}, \tag{4}$$

where K_{22}^* is the effective twist elastic constant, which can be expressed as

$$K_{22}^* = K_{22}\left(1 - \frac{\xi}{d}\right). \quad (5)$$

4. Conclusions

A surface interaction effect has been discussed in an electrically induced cholesteric-nematic (Ch-N) phase transition. A relatively short helical pitch liquid crystal compared to a cell thickness shows a strong dependence of the threshold electric field on the cell thickness in a homeotropically aligned cell. The strong surface interaction results in the bistable memory effect. In the cholesteric to nematic phase transition, the anchoring energy, A_θ, contributes to reduce the threshold electric field; in particular the cell thickness is less than 5 μm. Our expression of the threshold electric field, taking into account the surface contribution suggests that in the homeotropically aligned cell using the silane coupling agent (DMOAP), A_θ is on the order of 10^{-4} J/m^2.

In the N to Ch phase transition, the surface interaction is assumed to have an effect on the twist elastic constant. A distorted helical structure at the surface may modulate K_{22}. Consequently, the effective twist elastic constant K_{22}^* behaves as $K_{22}^* < K_{22}$. Thus the threshold electric field from a nematic to cholesteric reduces with the reduction of the relative influence of the surface interaction, which is substituted by the cell thickness, d.

APPENDIX

Threshold electric fields of the Ch-N phase transition taking into account the surface effects.

As soon as the electric field strength reaches a certain threshold value, the system becomes a nematic phase that is, the period p of the helix diverges at this critical field strength. The helix axis is taken along the z axis and the applied field along with the y axis. The director field is given by

$$n = [\sin\theta(z), \cos\theta(z), 0)].$$

First of all, to obtain the function $\theta(z)$, the free energy per unit volume is minimized. The free energy per unit volume, taking into account the twist term and the surface energy, A_θ, is given by

$$F = \frac{1}{2}\int_0^d \int_0^{P(E)} \left[K_{22}\left(\frac{\partial\theta}{\partial x} - t_0\right)^2 - \varepsilon_0\Delta\varepsilon E^2(1 - \sin^2\theta) + \frac{1}{2}A_\theta(1 - \sin^2\theta) - \frac{1}{2}K_{22}t_0^2\right] dx\, dz. \quad (6)$$

In Equation (6), $\partial\theta/\partial z = 0$ and $\int dz = d$, which means that the integration along the z direction leads to the LC layer thickness, d. The function $\theta(z)$ follows from the requirement that the energy F must be stationary. Consequently $\theta(z)$ must satisfy the Euler-Lagrange Equation

$$G^2 \frac{d^2\theta}{dx^2} + \sin\theta\cos\theta = 0 \tag{7}$$

with

$$G^2 = \frac{K_{22}}{\varepsilon_0 \Delta\varepsilon E^2 + \dfrac{2A_\theta}{d - \xi}}.$$

Where ξ is the thickness of the unwound layer of the helical structure. Multiplying (7) by $d\theta/dx$ and integrating yields

$$G\frac{d\theta}{dx} = \sqrt{C - \sin^2\theta}. \tag{8}$$

That is

$$x = G\int_0^\theta \frac{d\theta}{\sqrt{C - \sin^2\theta}}. \tag{9}$$

The dependence of the period $P(E)$ on the integrating constant C is given by

$$P(E) = \int_0^P dx = \int_0^{\pi/2} \frac{dx}{d\theta}\, d\theta = \int_0^{\pi/2} \frac{d\theta}{\sqrt{C - \sin^2\theta}}. \tag{10}$$

The value $C = 1$ is a critical value, because then the period diverges. The next step is the calculation of the integration constant C as a function of E. To obtain C, Equation (8) is substituted for Equation (6), then minimizing F with respect to C gives the condition $dF/dC = 0$,

$$F = \frac{t_0^2 K_{22}}{2}\int_0^d\int_0^{2\pi} d\theta\left[\frac{2}{t_0^2}\left(\frac{\partial\theta}{\partial x}\right)^2 - \frac{2}{t_0}\frac{\partial\theta}{\partial x} + 1 - \frac{C}{G^2 t_0^2} + \frac{1}{t_0^2 K_{22}}\right.$$
$$\left.\cdot\left[\left(\varepsilon_0\Delta\varepsilon E^2 - \frac{1}{2}A\theta\right)\sin^2\theta - \varepsilon_0\Delta\varepsilon E^2 + \frac{1}{2}A_\theta - \frac{1}{2}K_{22}t_0^2\right]\right]\frac{dz}{d\theta}\,dx. \tag{11}$$

This means that the dependence of C on E is obtained by solving

$$\int_0^{\pi/2} d\theta\sqrt{C - \sin^2\theta} = \frac{\pi}{2}Gt_0^2. \tag{12}$$

This Equation determines a threshold value for the applied electric field, because it does not allow a solution for C as soon as the field strength exceeds a critical value. The lowest possible value for C is $C = 1$. Consequently the critical field value is given by

$$\int_0^{\pi/2} d\theta\sqrt{C - \sin^2\theta} = \int_0^{\pi/2} d\theta \cos\theta = 1 = \frac{\pi}{2} G t_0 = \frac{\pi^2 G}{P_0}. \tag{13}$$

Then the following relation is obtained,

$$\frac{1}{G^2} = \left(\frac{\pi}{P_0}\right)^2 = \frac{\varepsilon_0 \Delta\varepsilon E^2 + \dfrac{2A_\theta}{d - \xi}}{K_{22}}. \tag{14}$$

Thus,

$$E^2 = \left(\frac{\pi^2}{P_0}\right)\frac{K_{22}}{\varepsilon_0\Delta\varepsilon} - \frac{2A_\theta}{\varepsilon_0\Delta\varepsilon(d - \xi)}. \tag{15}$$

Here, de Gennes Equation[16]

$$E_{CN} = \frac{\pi_2}{P_0}\sqrt{\frac{K_{22}}{\varepsilon_0\Delta\varepsilon}}$$

is substituted for Equation (15), the cholesteric to nematic threshold field

$$E^*_{CN} = \sqrt{E^2_{CN} - \frac{2A_\theta}{\varepsilon_0\Delta\varepsilon(d - \xi)}}, \tag{16}$$

is obtained.

References

1. J. J. Wysocki, A. Adams and W. Haas, *Phys. Rev. Lett.*, **20**, 1024 (1968).
2. G. H. Heilmeir and J. E. Goldmacher, *Appl. Phys. Lett.*, **13**, 132 (1968).
3. D. L. White and G. N. Taylor, *J. Appl. Phys.*, **45**, 4718 (1974).
4. W. R. Heffner and D. W. Berreman, *J. Appl. Phys.*, **53**, 8599 (1982).
5. M. Kawachi, K. Kato and O. Kogure, *Jpn. J. Appl. Phys.*, **16**, 1263 (1977).
6. M. Kawachi, K. Kato and O. Kogure, *Jpn. J. Appl. Phys.*, **16**, 1673 (1977).
7. C. G. Lin-Hendel, *Appl. Phys. Lett.*, **38**, 615 (1981).
8. C. G. Lin-Hendel, *J. Appl. Phys.*, **53**, 916 (1982).
9. P. R. Gerber, *Z. Naturforsch. Teil A*, **38**, 407 (1983).
10. F. Gharadjedaghi, *Mol. Cryst. Liq. Cryst.*, **68**, 127 (1981).
11. J. C. Lee, D. W. Allender and D. Neff, *Mol. Cryst. Liq. Cryst.*, **210**, 11 (1992).
12. H. A. van Sprang and J. L. M. van de Venne, *J. Appl. Phys.*, **57**, 175 (1985).
13. A. Mochizuki, H. Gondo, T. Watanuki, K. Saito, K. Ikegami and H. Okuyama, *Proceedings of the SID (Society for Information Display)*, **26**, 243 (1985).

14. A. Mochizuki, M. Iwasaki, Y. Yamagishi, H. Gondo and H. Yamaguchi, *Proceedings of SPIE—The International Society for Optical Engineering*, **760**, 74 (1987).
15. A. Mochizuki, T. Yoshihara, M. Iwasaki, Y. Yamagishi, Y. Koike, M. Haraguchi and Y. Kaneko, *Proceedings of the SID* **31**, 155 (1990).
16. P. G. de Gennes, *Sol. State Comm.*, **6**, 168 (1968).
17. W. Greubel, *Appl. Phys. Lett.*, **25**, 5 (1974).